Proceedings of SOLAR 2002
Sunrise on the Reliable Energy Economy
June 15 – 20, Reno, Nevada

THEORETICAL ANALYSIS OF AMMONIA-BASED COMBINED POWER/REFRIGERATION CYCLE AT LOW REFRIGERATION TEMPERATURES

Shaoguang Lu and **D. Yogi Goswami**
Solar Energy and Energy Conversion Laboratory
Department of Mechanical Engineering
University of Florida, PO Box 116300
Gainesville, FL 32611-6300
Email: solar@cimar.me.ufl.edu

ABSTRACT

A new combined power/refrigeration cycle uses ammonia/water mixture as a working fluid to produce both power and refrigeration in the same cycle. The cycle may be designed for various combinations of power and refrigeration. In an earlier paper by the authors, the cycle was optimized for efficiency, with power as the main intended output. This study puts an emphasis on the refrigeration part of the total output especially at low refrigeration temperatures. The objective was to find out what kind of outputs could be obtained at very low temperatures for a possible application in the Mars mission. The thermal performance of this cycle at different refrigeration temperatures has been found. At each refrigeration temperature, the cycle is optimized for maximum second law efficiency using Generalized Reduced Gradient (GRG) algorithm. It is found that refrigeration temperatures as low as 205 K may be achieved using this cycle. Generally, both first and second law efficiencies decrease when refrigeration temperature drops. For a re-circulating type of solar thermal system with a source temperature of 360K, the first and second law efficiencies increase slightly as the refrigeration temperature goes down from 265K to 245K and then decrease with the refrigeration temperature, giving a maximum second law efficiency of 63.7% at 245K.

INTRODUCTION

Recently, alternative power cycles employing multi-component working fluids have been studied intensively. The motivation for using mixtures is that heat transfer occurs at variable temperatures thus providing a better thermal match between a sensible heat source and the working fluid.

A well known thermodynamic power cycle using ammonia-water mixture as the working fluid is Kalina cycle [1]. A comparison of the Kalina cycle to the Rankine cycle by El-Sayed and Tribus shows a 10% to 20% improvement in thermal efficiency [2]. Marston [3], Park and Sonntag [4], and Ibrahim and Klein [5] also analyzed the Kalina cycle and showed advantages of the Kalina cycle over the conventional Rankine cycle under certain conditions.

Goswami [6, 7] proposed a new combined power/refrigeration cycle using ammonia-water mixtures as working fluids. The cycle takes advantage of the varying boiling temperatures of the ammonia/water mixtures to get a better thermal match with a sensible heat source. It also takes advantage of the low boiling temperature of ammonia vapor to provide refrigeration even though power is the primary goal. This cycle may be designed as a bottoming cycle utilizing waste heat from a conventional power cycle or as an independent cycle using low temperature sources such as geothermal and solar energy.

The proposed cycle is shown schematically in Fig. 1. Referring to this figure, the ammonia-water strong solution is pumped from the absorber to a high pressure at state 2. At this point, the solution is split into two streams. One stream goes through a heat exchanger (state 2') to recover heat from the weak solution exiting from the boiler. The second stream goes to the rectifier (state 2") to cool the ammonia vapor exiting the boiler to condense the water vapor in it. The two streams are combined again (state 3) before entering the boiler. In the boiler, the mixture is heated to boil off ammonia vapor (state 4). In order to get high concentration ammonia vapor (state 6), the vapor goes through the rectifier to condense some water in it. The condensate is rich in water and returns to the boiler (state 5). The enriched ammonia vapor is then superheated in a superheater (state 7). After expansion in the turbine, ammonia vapor drops to a very low temperature (state 8). The low temperature ammonia vapor provides cooling by passing through the refrigeration heat exchanger (state 9). Ammonia vapor is then absorbed into the weak solution in the absorber to regenerate the ammonia-water strong solution (state1). Weak solution leaving the boiler (state 10) goes through a heat recovery heat exchanger (state 11) to transfer heat to the strong solution. After passing through a pressure-reducing valve (state 12), the weak solution returns to the absorber.

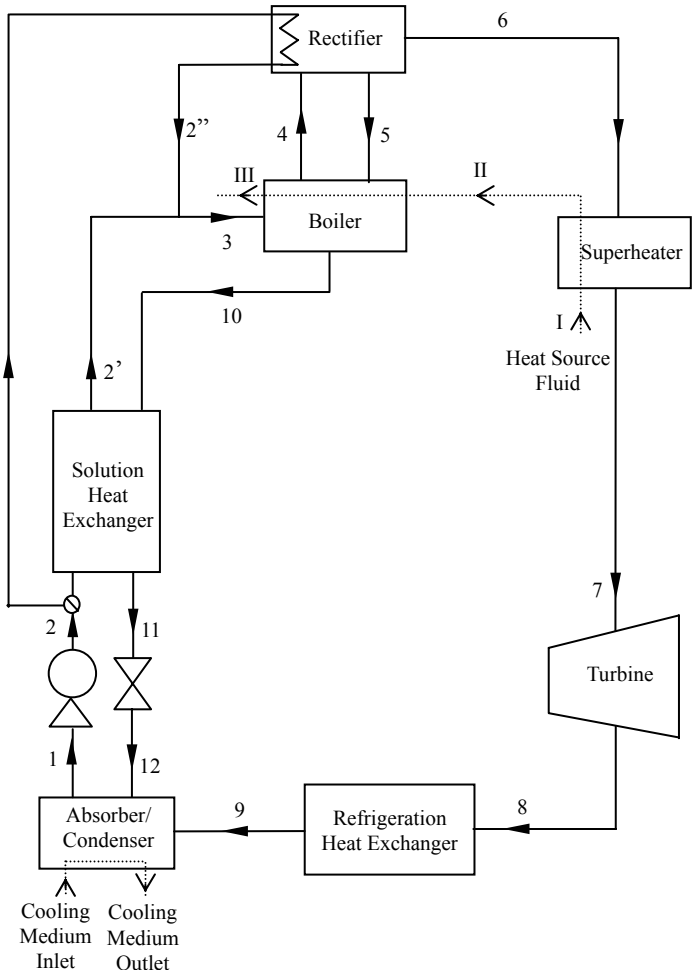

Fig. 1 Ammonia-Based Combined Power /Refrigeration Cycle

A parametric study of the cycle was conducted by Goswami and Xu [8]. The results revealed that the cycle has good potential for production of power and refrigeration at the same time and can be optimized for the best performance. A first law efficiency of 23.54% was achieved for the cycle for a heat source temperature of 410 K and an absorber temperature of 280 K. Lu and Goswami [9] presented a mathematical optimization technique to optimize the operating conditions of the cycle for the best thermal performance for various heat source and sink conditions.

This paper analyzes the performance of the cycle at low refrigeration temperatures. At each refrigeration temperature, the cycle is optimized for maximum second law efficiency. The objective of this study was to analyze the output of the cycle while achieving very low refrigeration temperatures for a possible application in the Mars mission. We were also interested in finding out the lowest temperature achievable by this cycle using ammonia/water as working fluid.

NOMENCLATURE

COP_{ideal} = Ideal coefficient of performance

P_{high} = Cycle high pressure, bar

P_{low} = Cycle low pressure, bar

P_x = Working fluid pressure at point x (refer to Fig. 1), bar

$\dot{Q}_{absorber}$ = Absorber heat rejection rate, kJ/s

$\dot{Q}_{boiler}$ = Boiler heat input rate, kJ/s

$\dot{Q}_{cool}$ = Refrigeration output, kJ/s

$\dot{Q}_{rectifier}$ = Rectifier heat transfer rate, kJ/s

$\dot{Q}_{superheater}$ = Superheat input rate, kJ/s

T_0 = Ambient temperature, K

$T_{absorber}$ = Absorber temperature, K

T_{boiler} = Boiler temperature, K

$T_{rectifier}$ = Rectifier temperature, K

$T_{superheater}$ = Superheater temperature, K

$T_{boilermin}$ = Minimum boiler temperature, K

$T_{rectifiermin}$ = Minimum rectifier temperature, K

T_{hs}^{in} = Heat source inlet temperature, K

T_{hs}^{out} = Heat source exit temperature, K

T_x = Working fluid temperature at point x, K

T_I = Heat source temperature at I, K

T_{II} = Heat source temperature at II, K

T_{III} = Heat source temperature at III, K

ΔT_{min} = Minimum temperature difference required in the heat exchangers, K

ΔT_{pin} = Temperature difference at pinch point in the boiler, K

ΔT_{pin}^{min} = Minimum temperature difference required at pinch point, K

W_{net} = Net power output , kW

W_p = Pump work input, kW

W_t = Turbine work output, kW

X = Mass fraction of ammonia in the working fluid, kg ammonia/kg mixture

$f_{2"}$ = Mass fraction at point 2"

f_4 = Mass fraction at point 4

h_0 = Specific enthalpy of the heat source fluid at ambient temperature, kJ/kg

h_{hs}^{in} = Heat source inlet specific enthalpy, kJ/kg

h_{hs}^{out} = Heat source outlet specific enthalpy, kJ/kg

h_x = Working fluid specific enthalpy at point x, kJ/kg

$\dot{m}_{hs}$ = Mass flow rate of the heat source fluid, kg/s

$\dot{m}_x$ = Mass flow rate of the working fluid at point x, kg/s

s_0 = Specific entropy of the heat source fluid at ambient temperature, kJ/kg.K

s_{hs}^{in} = Heat source inlet specific entropy, kJ/kg.K

s_{hs}^{out} = Heat source outlet specific entropy, kJ/kg.K

s_x = Working fluid specific entropy at point x, kJ/kg.k

$x_{turbine}$ = Vapor quality at turbine exit

η_1 = First law thermal efficiency

η_2 = Second law thermal efficiency

THERMODYNAMIC ANALYSIS

The ammonia-based combined power/refrigeration cycle produces power output as well as refrigeration even though power generation may be the primary goal. Lu and Goswami [9] used a well-developed optimization algorithm to find the optimum working conditions for the cycle which showed that both power and refrigeration output were obtained. However, that study did not analyze the effect of refrigeration temperature on the cycle performance. It is known that in general the refrigeration output from a refrigeration cycle is reduced when the required refrigeration temperature is reduced. This study was conducted to find out if lower refrigeration temperatures give lower refrigeration output for this cycle and also to see how lower refrigeration temperatures may affect the power output.

Thermodynamic Properties of Ammonia Water Mixtures

Ammonia-water mixtures have been used in absorption refrigeration cycles for several decades. Their thermophysical properties are readily available over the temperature and pressure range of absorption refrigeration cycles. The properties of ammonia-water mixtures have been extended to a wider range in recent years in order to study their use in power cycles.

The method presented by Xu and Goswami [10] is used to calculate the properties of ammonia-water mixtures in this simulation. This method uses Gibbs free energy equations for pure ammonia and water properties, and empirical bubble and dew point temperature equations for vapor-liquid equilibrium. It covers a pressure range of 0.2 to 110 bars and a temperature range of 230 to 600K. The method gives results consistent with the available experimental data.

Second Law Analysis

Second law analysis has been employed extensively to analyze the thermodynamic power cycles in the literature. However, there is limited amount of published literature on the second law analysis of refrigeration cycles. Lee and Sherif [11] analyzed multi-stage lithium bromide/water absorption heat transformers by the second law in conjunction with the first law analysis. They defined second law efficiency in two ways. The first definition is the ratio of the Coefficient of Performance (COP) of the real cycle to the COP of an ideal cycle. COP is defined as the ratio of useful refrigeration obtained from a system to the energy input to the system. The second method defines the second law efficiency as the ratio of the useful exergy gained from a system to that supplied to the system. Krakow [12] and Alefeld [13] suggested a similar method to calculate the second law efficiency.

The first law efficiency is defined as the useful energy output from a cycle to the energy input to the cycle. For the combined power/refrigeration cycle, it is expressed as:

$$\eta_1 = \frac{W_{net} + \dot{Q}_{cool}}{\dot{m}_{hs}(h_{hs}^{in} - h_{hs}^{out})} \tag{1}$$

Where W_{net} is the net power output;

$\dot{Q}_{cool}$ is the refrigeration output;

$\dot{m}_{hs}$ is the mass flow rate of the heat source fluid;

h_{hs}^{in} is the inlet specific enthalpy of the heat source fluid;

h_{hs}^{out} is the outlet specific enthalpy of the heat source fluid.

The second law efficiency may be defined as the ratio of the useful energy output from the cycle to the exergy consumption of the cycle. Hasan and Goswami [14] gave a definition of the second law efficiency as:

$$\eta_2 = \frac{W_{net} + \dot{Q}_{cool} / COP_{ideal}}{\dot{m}_{hs}[(h_{hs}^{in} - h_{hs}^{out}) - T_0(s_{hs}^{in} - s_{hs}^{out})]} \tag{2}$$

Where COP_{ideal} is the coefficient of performance for an ideal refrigeration cycle;

T_0 is the ambient temperature;

s_{hs}^{in} is the inlet specific entropy of the heat source fluid; and

s_{hs}^{out} is the outlet specific entropy of the heat source fluid.

The denominator is the exergy change of the heat source fluid. This definition assumes that the spent heat source fluid is reheated in a closed loop solar energy system. Equation (2) divides the refrigeration output by the ideal COP to find its power equivalent in the numerator. It plays down the significance of the refrigeration output in the cycle. Optimization for the maximum η_2 according to equation (2) tends to sacrifice the refrigeration output to produce more power output. In this equation, refrigeration is given a weight of $1/COP_{ideal}$ as compared to 1 for power. This definition would be fine when power output is the major intended output. If, however, refrigeration output, especially at low temperatures, is the major intended output, the weight given to the refrigeration output needs to be reconsidered. If the refrigeration output is given a weight equal to the power output, the second law efficiency becomes:

$$\eta_2 = \frac{W_{net} + \dot{Q}_{cool}}{\dot{m}_{hs}[(h_{hs}^{in} - h_{hs}^{out}) - T_0(s_{hs}^{in} - s_{hs}^{out})]} \tag{3}$$

If for the heat source fluid that is disposed off after transferring heat to the working fluid, for example, in geothermal energy applications, the denominator in equation (3) is changed to the inlet exergy of the heat source:

$$\eta_2 = \frac{W_{net} + \dot{Q}_{cool}}{\dot{m}_{hs}[(h_{hs}^{in} - h_0) - T_0(s_{hs}^{in} - s_0)]} \quad (4)$$

Where h_0 is the specific enthalpy of the heat source fluid at ambient temperature; s_0 is the specific entropy of the heat source fluid at ambient temperature.

Simulation and Optimization

Referring to Fig. 1, the thermodynamic simulation of the cycle consists of the following basic equations:

Boiler heat input:

$$\dot{Q}_{boiler} = \dot{m}_4 h_4 + \dot{m}_{10} h_{10} - \dot{m}_3 h_3 - \dot{m}_5 h_5 \quad (5)$$

Superheat input:

$$\dot{Q}_{superheater} = \dot{m}_6 (h_7 - h_6) \quad (6)$$

Rectifier heat transfer:

$$\dot{Q}_{rectifier} = \dot{m}_5 h_5 + \dot{m}_6 h_6 - \dot{m}_4 h_4 = \dot{m}_{2''}(h_2 - h_{2''}) \quad (7)$$

Absorber heat rejection:

$$\dot{Q}_{absorber} = \dot{m}_1 h_1 - \dot{m}_{12} h_{12} - \dot{m}_9 h_9 \quad (8)$$

Pump work input:

$$W_p = \dot{m}_1 (h_2 - h_1) \quad (9)$$

Turbine work output:

$$W_t = \dot{m}_7 (h_7 - h_8) \quad (10)$$

Refrigeration output:

$$\dot{Q}_{cool} = \dot{m}_8 (h_9 - h_8) \quad (11)$$

Where $\dot{m}_x$ is the mass flow rate of the working fluid at point x, and h_x is the specific enthalpy of the working fluid at point x.

To study the effect of the refrigeration temperature on the cycle performance, the cycle is optimized for maximum second law efficiency at each refrigeration temperature. A generalized reduced gradient (GRG) algorithm as described in Lu and Goswami (2001) and other references [15 – 17] is used.

This combined power/refrigeration cycle has eight free variables: the absorber temperature $T_{absorber}$, the boiler temperature T_{boiler}, the rectifier temperature $T_{rectifier}$, the superheater temperature $T_{superheater}$, the high pressure P_{high}, the low pressure P_{low}, the heat source entrance temperature T_{hs}^{in}, and the heat source exit temperature T_{hs}^{out}. Each combination of the eight values represents a distinct operating condition of the cycle. The objective function for the optimization of the cycle can be written as:

$$\eta_2 = f(T_{absorber}, T_{boiler}, T_{rectifier}, T_{superheater}, P_{high}, P_{low}, T_{hs}^{in}, T_{hs}^{out}) \quad (12)$$

To maintain the practicability of the cycle, a set of constraints is required to define a feasible region for the optimization search:

$$T_{boiler} \geq T_{rectifier}$$
$$T_{superheater} \geq T_{rectifier}$$
$$T_{boiler} \geq T_{boilermin}$$
$$T_{rectifier} \geq T_{rectifiermin}$$
$$x_{turbine} \geq 0.9$$
$$0 \leq f_4 \leq 1$$
$$0 \leq f_{2''} \leq 1$$
$$T_{10} - T_{2'} \geq \Delta T_{min}$$
$$T_I - T_{supheater} \geq \Delta T_{min}$$
$$T_{II} - T_{boiler} \geq \Delta T_{min}$$
$$T_{III} - T_3 \geq \Delta T_{min}$$
$$\Delta T_{pin} \geq \Delta T_{pin}^{\min}$$

Where $T_{boilermin}$ is the minimum boiler temperature;

$T_{rectifiermin}$ is the minimum rectifier temperature;

$x_{turbine}$ is the vapor quality at turbine exit;

f_4 is the mass fraction at point 4, defined as m_4/m_1;

$f_{2''}$ is the mass fraction at point 2", defined as $m_{2''}/m_1$;

T_x is the temperature at state point x (refer to Fig. 1);

T_I, T_{II} and T_{III} are the heat source temperature at point I, II, and III, respectively.

ΔT_{min} is the minimum temperature difference required in the heat exchangers;

ΔT_{pin} is the temperature difference at pinch point in the boiler;

$\Delta T_{pin}^{\min}$ is the minimum temperature difference required at pinch point.

To fix the refrigeration temperature, a new constraint is added into the existing constraints set:

T_8 = fixed value;

Results and Discussion

The analysis is done for a 360K heat source temperature, which is within the range of flat-plate solar collectors and solar ponds, and 290K as the ambient temperature. Refrigeration temperatures from 265K and below are considered. The simulation starts with a refrigeration temperature of 265K, decreasing it by 10K every time, until no power and refrigeration is produced by the cycle. However, since the thermophysical property program only covers down to 230K, uncertainty exists below that temperature. Keeping in mind, the results below 230K presented here should be looked at only for their qualitative significance.

The optimization results for the cycle at 265K refrigeration temperature based on equation (2) are given in tabular form to provide detailed property data at each state point and the

energy input and output quantities in the cycle. Table 1 shows the optimum working conditions. X is the mass fraction of ammonia in the working fluid. Table 2 gives the cycle performance parameters at the optimum working conditions.

Table 1 Optimum Working Conditions for Heat Source of 360K, Ambient Temperature 290K and Refrigeration Temperature 265K

Point	T(K)	P(bar)	h(kJ/kg)	s(kJ/kg.K)	X	Flow Rate (kg/s)
1	295.0	0.439	-56.8	0.2990	0.2253	1.0000
2	295.0	2.759	-56.6	0.2990	0.2253	1.0000
3	347.0	2.759	200.0	1.0910	0.2253	1.0000
4	355.0	2.759	1666.9	5.9235	0.8232	0.0779
5	331.2	2.759	65.7	0.7568	0.2887	0.0159
6	331.2	2.759	1455.8	5.4536	0.9598	0.0621
7	331.2	2.759	1455.8	5.4536	0.9598	0.0621
8	265.0	0.439	1199.2	5.4536	0.9598	0.0621
9	285.0	0.439	1310.2	5.8529	0.9598	0.0621
10	355.0	2.759	226.9	1.1114	0.1766	0.9379
11	300.0	2.759	-5.6	0.3998	0.1766	0.9379
12	300.1	0.439	-5.6	0.4006	0.1766	0.9379

Table 2 Cycle Performance Parameters For Conditions In Table 1

Boiler Heat Input:	141.7 kJ/s
Absorber Heat Rejection:	132.9 kJ/s
Turbine Work Output:	15.9 kW
Vapor Quality at Turbine Exit:	94.33 %
Pump Work Input:	0.3 kW
Refrigeration Capacity:	6.9 kW
Total Heat Input:	141.7 kJ/s
Total Work Output:	15.68kW
First Law Efficiency:	15.93 %
Second law efficiency:	62.18 %

The optimization results based on equation (2) are presented graphically in figures 2 to 6. Figure 2 gives the variation of first and second law efficiencies with the refrigeration temperature. It shows that when the refrigeration temperature goes down, both first and second law efficiencies increase slightly at first, and then drop. Both first and second law efficiencies have a maximum at a refrigeration temperature of 245K. The first law efficiency has a maximum of 17.41% and the second law efficiency has a maximum of 63.7%. The figure also shows that the first and second law efficiencies approach zero at 205K refrigeration temperature.

Figure 3 shows the variation of the absorber and turbine inlet pressures with refrigeration temperature. When the refrigeration temperature drops from 265K to 205K, both the absorber and the turbine inlet pressure first increase and then decrease below 245K refrigeration temperature.

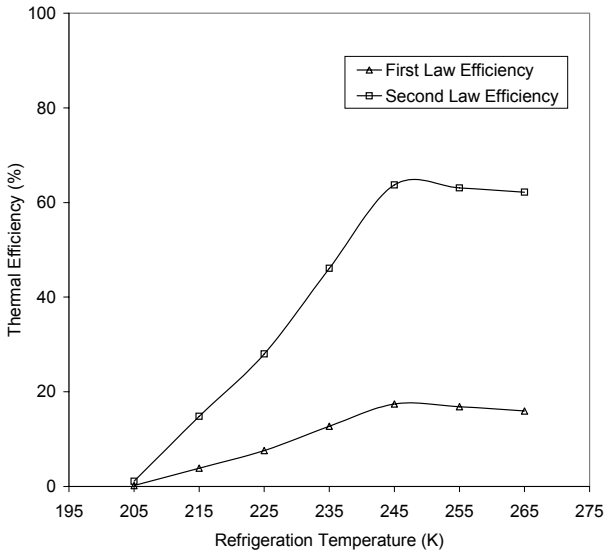

Fig. 2 Optimum First and Second Law Efficiencies at Different Refrigeration Temperatures Based on Maximizing Equation (2)

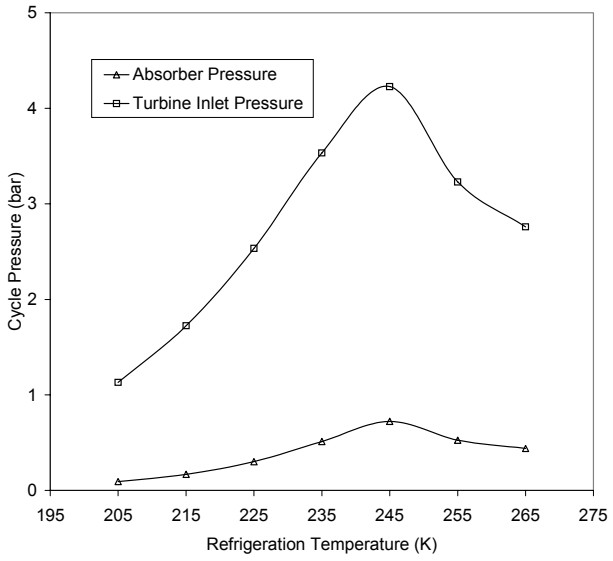

Fig. 3 Optimum Cycle Pressures at Different Refrigeration Temperatures Based on Maximizing Equation (2)

Figure 4 shows that the concentration of the ammonia solution in the absorber (mass fraction) increases at first as the refrigeration temperature decreases, and then decreases. Figure 5 shows that the ammonia vapor fraction increases slightly as the refrigeration temperature drops from 265K to 245K, and then decreases for refrigeration temperature below 245K.

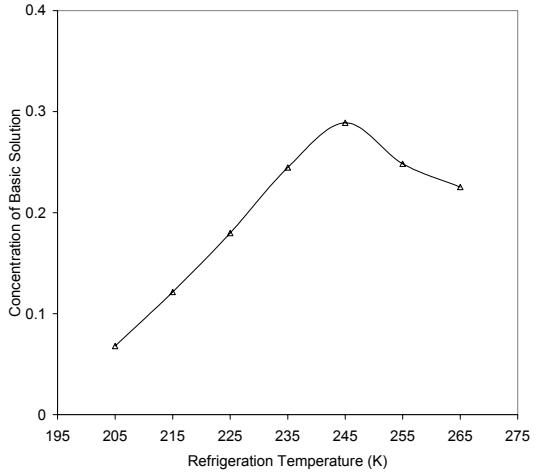

Fig. 4 Optimum Concentration of Basic Solution at Different Refrigeration Temperatures Based on Maximizing Equation (2)

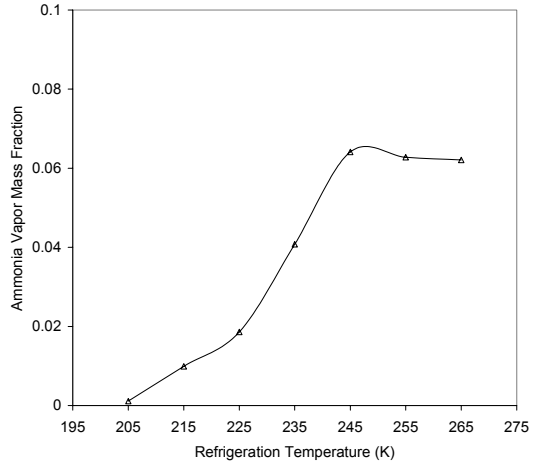

Fig. 5 Optimum Ammonia Vapor Mass Fraction at Different Refrigeration Temperatures Based on Maximizing Equation (2)

Figure 6 shows the variation of normalized work output and refrigeration output with refrigeration temperature. Generally, normalized work and refrigeration outputs increase. However, COP of the ideal refrigeration cycle has higher values at higher refrigeration temperatures. Therefore, when the refrigeration temperature is above 245K, the ideal COP is so large that the contribution of the refrigeration output to the second law efficiency becomes very small. Consequently, optimization reduces the refrigeration output to obtain a slight increase in the work output. Therefore, refrigeration output starts to drop when the refrigeration temperature goes above 245K.

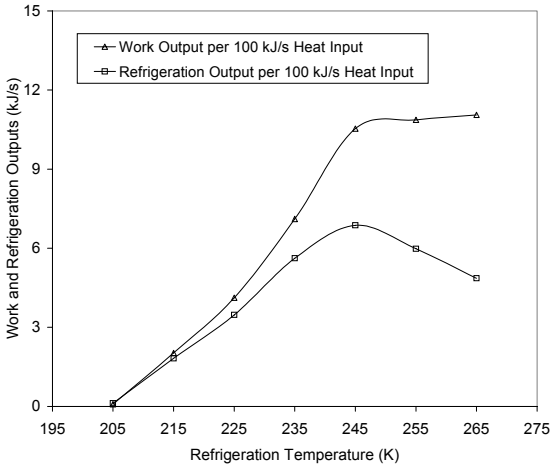

Fig. 6 Optimum Work and Refrigeration Outputs at Different Refrigeration Temperatures Based on Maximizing Equation (2)

Since refrigeration is the main intended output in this study, the cycle was also optimized for the second law efficiency in equation (4) where refrigeration is given a weight equal to the power output. The optimization results based on equation (4) are presented graphically from figures 7 to 11. Figure 7 shows the variation of the second law efficiency with refrigeration temperature. Unlike the results shown in Fig. 2, the second law thermal efficiency of the cycle based on equation (4) always decreases as refrigeration temperature goes down. At 265K, the cycle has a second law thermal efficiency of 52.2%, and it decreases as refrigeration temperature goes down. It approaches zero at 205K refrigeration temperature. The first law efficiency of the cycle also decreases with the refrigeration temperature.

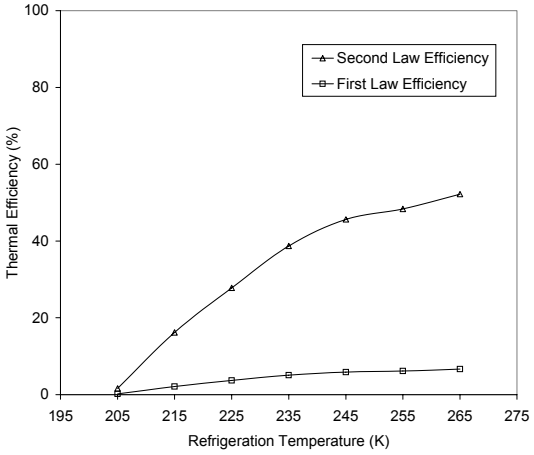

Fig. 7 Optimum First and Second Law Efficiencies at Different Refrigeration Temperatures Based on Maximizing Equation (4)

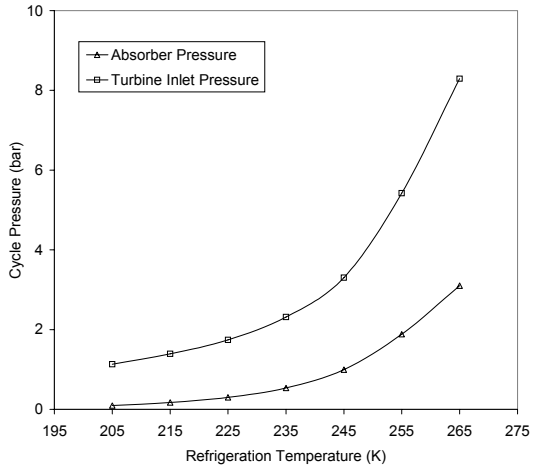

Fig. 8 Optimum Cycle Pressures at Different Refrigeration Temperatures Based on Maximizing Equation (4)

Figure 8 shows the variation of the absorber and turbine inlet pressures with refrigeration temperature. Starting at 265K, the absorber pressure decreases with refrigeration temperature while it shows a peak in Fig. 3. When refrigeration temperature goes lower, in order to maintain the quality level of the ammonia vapor at the exit of the turbine, the exhaust pressure of the turbine has to be lowered correspondingly. Under idealized conditions, the absorber pressure is equal to the turbine exhaust pressure and therefore is lower at low refrigeration temperatures. The turbine inlet pressure also decreases with refrigeration temperature. When the concentration of ammonia basic solution gets lower at a low refrigeration temperature, in order to produce enough ammonia vapor in the boiler, the boiler pressure has to go down correspondingly. Since turbine inlet pressure is the same as the boiler pressure under idealized conditions, it goes down simultaneously.

Figure 9 shows a variation of the concentration of the ammonia solution in the absorber with the refrigeration temperature. Compared with Fig. 4, it is found that the optimal basic solution concentration based on equation (4) has no peak. It decreases when the refrigeration temperature decreases. In order to generate as much ammonia vapor in the boiler as possible, a saturation state for ammonia solution is desired in the absorber. For saturated ammonia solution, its concentration is determined by its temperature and pressure. When the temperature is lower or the pressure is higher, the concentration of the saturated ammonia solution is higher. However, the temperature of the absorber is bounded by the ambient temperature. In this analysis, 5K above the ambient temperature is chosen for the absorber. So the concentration of the ammonia basic solution is only decided by the absorber pressure. When absorber pressure decreases with the refrigeration temperature, the concentration of the ammonia solution in the absorber also decreases with the refrigeration temperature. At 205K refrigeration temperature, the concentration of the basic solution at the optimum conditions is only 6.8%.

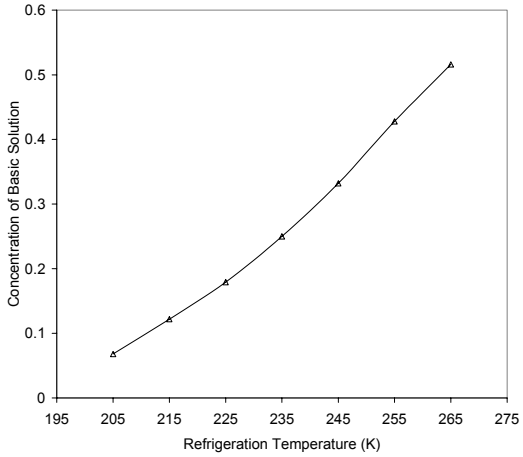

Fig. 9 Optimum Concentration of Basic Solution at Different Refrigeration Temperatures Based on Maximizing Equation (4)

Even though the boiler pressure goes down with the refrigeration temperature, the ammonia vapor generated in the boiler is very little at very low refrigeration temperatures due to the low concentration of the feeding ammonia solution. This point becomes clear from Fig. 10. The vapor fraction, which is the ratio of the mass flow rate of the ammonia vapor at point 6 to that of the ammonia basic solution at point 1, is almost zero at 205K refrigeration temperature. However, in Fig. 5, the vapor fraction reaches the maximum at 245K refrigeration temperature, where the concentration of the ammonia solution in the absorber is also the highest.

Figure 11 shows that turbine work output and refrigeration output (per kg/s heat source fluid) decrease with the refrigeration temperature. It is understandable that when less vapor flows through the turbine, less work and refrigeration will be produced. No peak appears for refrigeration output as in Fig. 6. The refrigeration curve shows an inflection point which seems odd. However, the results were confirmed by repeated simulations at points close to the inflection point. The inflection is believed to be caused by the nonmonotonous feature of the isobaric entropy curve of the saturated ammonia/water solution. When the mass concentration of the saturated ammonia/water solution increases, its entropy decreases but then increases after a minimum point. In the cycle, ammonia vapor becomes liquid/vapor mixture after expanding through the turbine. When refrigeration temperature varies from 245K to 265K across the inflection point, it was found that the entropy of the liquid ammonia/water in the mixture moves its position on the isobaric entropy curve from the left side of the minimum point to the right side.

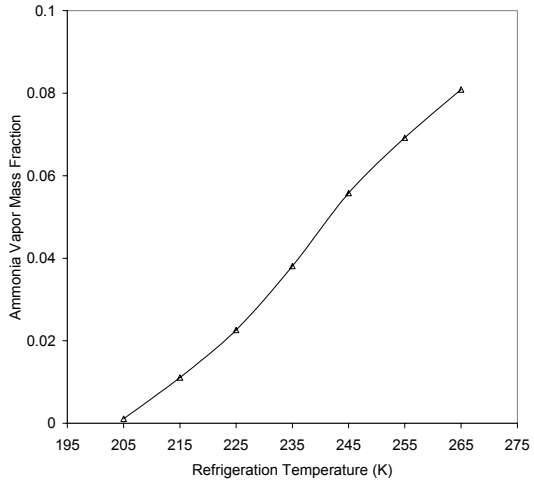

Fig. 10 Optimum Ammonia Vapor Mass Fraction at Different Refrigeration Temperatures Based on Maximizing Equation (4)

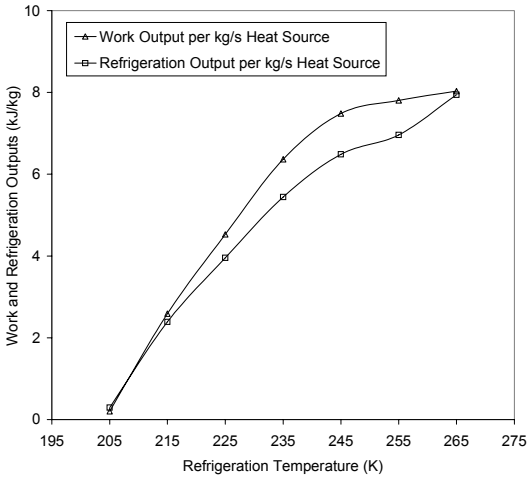

Fig. 11 Optimum Work and Refrigeration Outputs at Different Refrigeration Temperatures Based on Maximizing Equation (4)

CONCLUSIONS

The combined power and refrigeration thermodynamic cycle investigated in this paper can be used to produce refrigeration at low temperatures as well as power output. The performance of the cycle at low refrigeration temperature is studied in this paper. At each refrigeration temperature, operating conditions are established by maximizing a second law efficiency. Two slight different definitions of second law efficiency are employed. It is found that a refrigeration temperature as low as 205K could be achieved. However, the cycle performance generally worsens when the refrigeration temperature decreases. Both first and second law efficiencies therefore drop as the refrigeration temperature goes down. However, for one definition of second law efficiency, where the reciprocal of an ideal coefficient of performance is used as a weight factor for the refrigeration output, the first and second law efficiencies increase slightly as the refrigeration temperature decreases and then decrease, reaching maxima at 245K refrigeration temperature.

REFERENCES

1. Kalina A. I., 1983, "Combined Cycle and Waste-Heat Recovery Power Systems Based on a Novel Thermodynamic Energy Cycle Utilizing Low-Temperature Heat for Power Generation," ASME Paper 83-JPGC-GT-3.
2. El-Sayed Y. M., and Tribus M., 1985, "A Theoretical Comparison of the Rankine and Kalina Cycles," *ASME Special Publication*, **1**, pp. 97-102.
3. Marston C. H., 1990, "A Family of Ammonia-Water Adjustable Proportion Fluid Mixture Cycles," *Proceedings of the 25th Intersociety Energy Conversion Engineering Conference*, **2**, pp. 160-165.
4. Park Y. M., and Sonntag R. E., 1990, "A Preliminary Study of the Kalina Power Cycle in Connection with a Combined Cycle System," *Int. J. of Energy Res.*, **14**, pp. 153-162.
5. Ibrahim O. M., and Klein S. A., 1996, "Absorption Power Cycles", *Energy* (Oxford), **21**, pp. 21-27.
6. Goswami, D. Y., 1995, "Solar Thermal Power: Status of Technologies and Opportunities for Research," *Heat and Mass Transfer 95, Proceedings of the 2nd ASME-ISHMT Heat and Mass Transfer Conference*, Tata-McGraw Hill Publishers, New Delhi, India, pp. 57-60.
7. Goswami, D. Y., 1998, "Solar Thermal Power Technology: Present Status and Ideas for the Future," *Energy Sources*, **20**, pp. 137-145.
8. Goswami, D. Y., and Xu, F., 1999, "Analysis of a New Thermodynamic Cycle for Combined Power and Cooling Using Low and Mid Temperature Solar Collectors," *Journal of Solar Energy Engineering*, **121**, pp. 91-97.
9. Lu, S., Goswami, D. Y., 2001, "Optimization of a Novel Ammonia-Based Thermodynamic Cycle".
10. Xu, F., Goswami, D. Y., 1999, "Thermodynamic Properties of Ammonia Water Mixture for Use in Power Cycles," *Energy* (Oxford), **24**, pp. 525-536.
11. Lee, S. F., Sherif, S. A., 2000, "Second Law Analysis of Multi-Stage Lithium Bromide/Water Absorption Heat Transformers", *ASHRAE Transactions*, **106**, pp. 105-116.
12. Krakow, K. I., 1991, "Exergy Analysis. Dead-State Definition", *ASHRAE Transactions*, pt 1, pp. 328-336.

13. Alefeld, G., 1989, “Second Law Analysis for an Absorption Chiller”, *Newsletter of the IEA Heat Pump Center*, pp. 54-57.
14. Hasan, A. A., and Goswami, D. Y., 2001, “Exergy Analysis of a Combined Power and Refrigeration Thermodynamic Cycle Driven by a Solar Heat Source”.
15. Lasdon, L. S., Waren, A. D., Jain, A., Ratner, M., “Design and Testing of a Generalized Reduced Gradient Code for Nonlinear Programming”, *ACM Transactions on Mathematical Software*, **4**, pp.34-50.
16. Edgar T. F., and Himmelblau D.M., 1988, *Optimization of Chemical Processes*, McGraw-Hill, New York.
17. Hwang, C. L., Williams, J. L., and Fan, L.T., 1972, *Introduction to the Generalized Reduced Gradient Method*, Institute for Systems Design and Optimization, Manhattan.